Polyhedron 145 (2018) 154–165

Contents lists available at ScienceDirect

Polyhedron

journal homepage: www.elsevier.com/locate/poly

Review

Azamacrocyclic-based metal organic frameworks: Design strategies and applications

Chavis A. Stackhouse, Shengqian Ma *

Department of Chemistry, University of South Florida, Tampa, FL, United States

ARTICLE INFO

Article history:
Received 1 November 2017
Accepted 31 January 2018
Available online 8 February 2018

Keywords:
Metal organic frameworks
Coordination polymer
Azamacrocycle
Cyclen
Cyclam

ABSTRACT

Polyazamacrocycles and its functionalized derivatives have been employed recently as organic building blocks in the construction of extended metal–organic frameworks (MOFs). Incorporating azamacrocycles into the MOF architectures not only merges the chemistry of MOFs with supramolecular chemistry of the macrocycles, but also brings out novel properties from the hybrid frameworks produced. In this review, we describe recent advances of the fabrication of azamacrocycles into MOF structures along with the most prominent applications based upon azamacrocycle-containing MOFs, which include molecular recognition and separation, template synthesis, gas adsorption, and heterogenous catalysis.

Contents

1. Introduction

Owing to their unequaled potential tunability and structural diversity, metal-organic frameworks (MOFs) have attracted broad interests as an adaptable potential platform for a breadth of investigations in research ranging from exploring fundamental understandings of surface chemistry to applied research [1–10]. Characteristic high porosity and surface area displayed by MOFs cement the materials' promise for applied research; finding application in gas storage and separation [11–15], catalysis [16–19], sensing [20–22], proton conduction [23–26], and drug delivery [27–29]. As crystalline structures composed of metal ions or metal clusters of cations, commonly referred to as secondary building units (SBUs), and custom-designed organic ligands [30–32], the variety of structural motifs, ligands, and SBUs that could be incor-

* Corresponding author.
E-mail address: sqma@usf.edu (S. Ma).

https://doi.org/10.1016/j.poly.2018.01.036
0277-5387/

porated into the materials, encourage the realization of essentially countless potential MOFs. Further functionalization of MOF materials by means of post-synthetic modification (PSM) [33–37] of metal clusters or organic ligands, constructing frameworks using functional ligands or metal clusters, and incorporating advantageous molecules including organometallic molecules [38–41], enzymes [42–45], metal nanoparticles (NPs) [8,46–48], heteropolyacids [49–51] within the pores advance the diverse number of species, including organic ligands, inorganic metal ions/clusters, and guests, used to construct MOFs materials lead to MOFs materials possessing phenomenal properties. The modular variability of these materials highlights the researchers' abilities to engineer properties into MOFs following a bottoms-up approach, exploiting geometric, chemical, and electronic features presented in the organic and inorganic building blocks [52–56].

Polyazamacrocycles denote a popular class of macrocyclic ligands for supramolecular chemistry and crystal engineering. These ligands offer greater versatility than their crown ether analogs and other oxygen heteroatom containing macrocycles, e.g. cyclodextrins. Amines exhibit strong proton affinities due to greater basicity, may impart their lone pair electrons to Lewis acids, and may behave as strong Lewis acids which allows for their interaction with diverse anionic moieties via electrostatic interactions. The nitrogen heteroatom associates more strongly with transition metal ions than the oxygen heteroatom, shows capability to also coordinate to lanthanide metal ions, and its reduced electronegativity enhances the accessibility of lone pairs for complex formation. The saturated amine group may be modified to an imine, amide, or hydroxylamine moiety to increase complexity. Furthermore, the azamacrocycle may be employed as the macrocycle unit of a rotaxane moiety. The integration of this class of ligands in MOF structures lends the opportunity import N-donors, advance topological diversity, and impart the potential hierarchical porosity associated with macrocycles.

Complexes incorporating these ligands often exhibit a characteristic high thermodynamic stability and relative kinetic inertness, allowing for researchers to ignore any potential for dissociation in harsh MOF synthetic conditions. Furthermore, azamacrocycle complexes uniquely differ from other groups of macrocycles commonly employed in MOF synthesis through the macrocycle's capability to promote strong metal complexation during crystal synthesis which, whilst enhancing topological diversity [57–60], produces a metallated-azamacrocycle complex. This complex possesses a propensity to be regarded as a static structural moiety as it remains inert with respect to compositional changes during the formation of further coordination bonds to bridging ligands and supramolecular aggregates, but eliminates all activity of the macrocycle toward its reported applications upon its occupancy by various metal cations [61]. This strong coordination ability promotes interesting network topologies with an adroitness toward the purposeful design of frameworks with preconceived topology. The coordination interaction of tetradentate azamacrocycles promotes two possible types of conformational isomers; firstly, abundantly reported square planar equatorial N_4 coordination configurations (*trans*) which permits interaction at the remaining vacant trans-axial positions, and a folded conformation (*cis*) with two vacant cis positions, shown in Fig. 2. Amongst the possible *trans* configurations, types I, III, and IV, as identified using Bosnich terminology [63], are favored. Due to the abundance of *trans* configurations of similar energies, disorder of the macro-

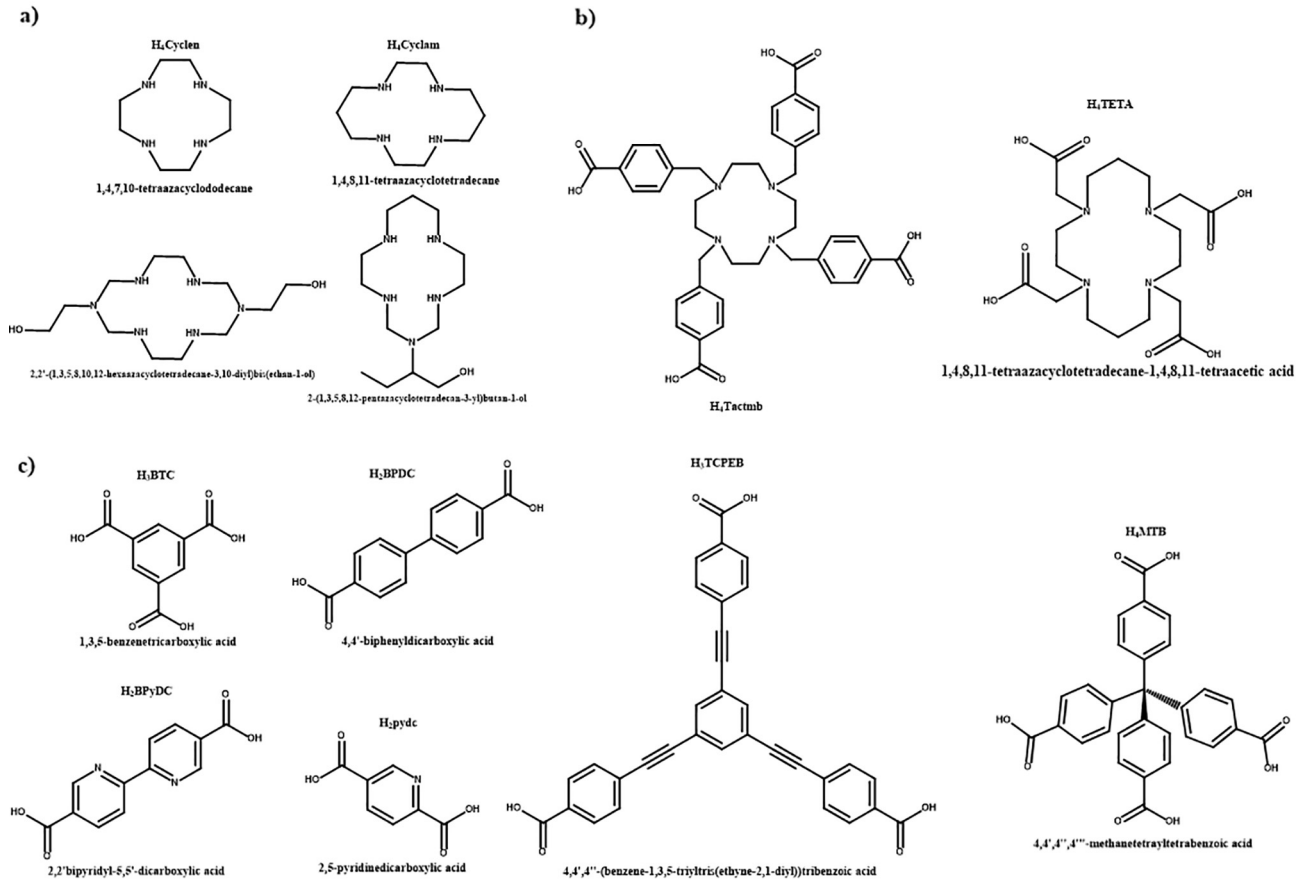

Fig. 1. (a) Azamacrocycles employed in metal complex linear linkers, (b) N-functionalized azamacrocycle ligands, and (c) Carboxylate co-ligands employed in the preparation of azamacrocyclic MOFs discussed in this article.

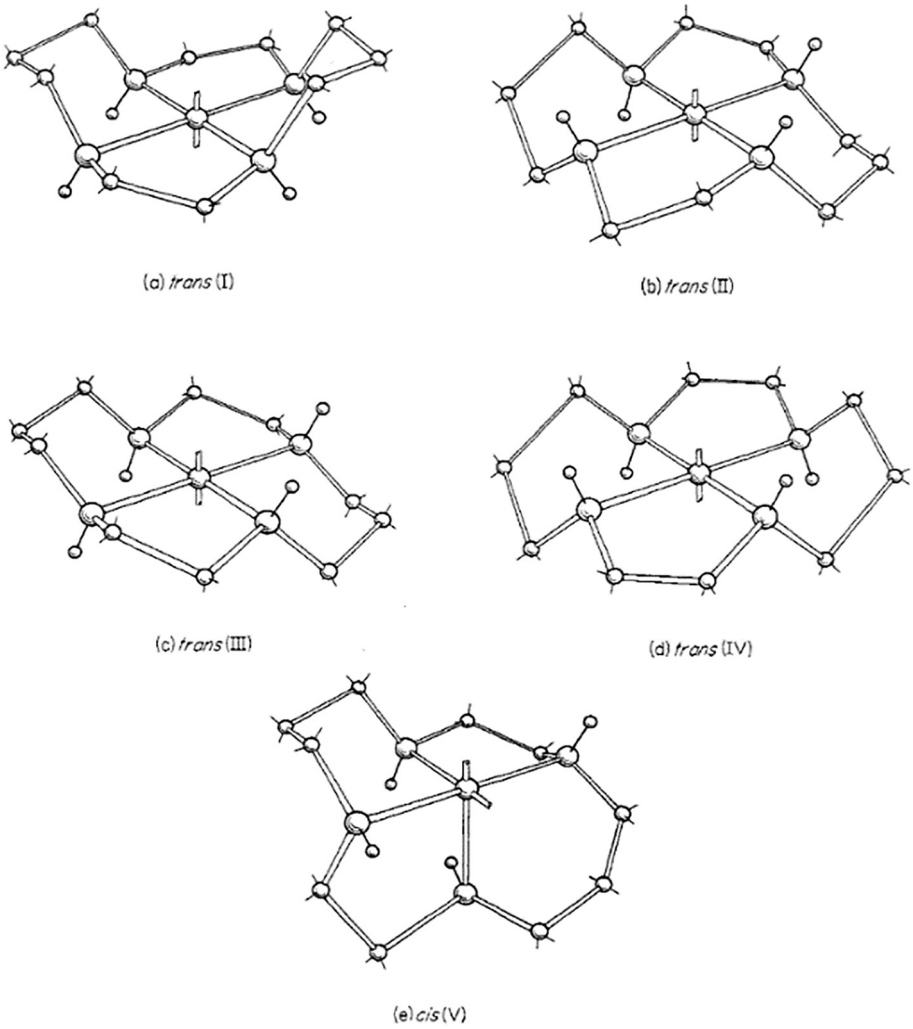

Fig. 2. Coordination configurations of N_4 azamacrocycles shown using Cyclam. Reprinted with permission from Ref. [63]. Copyright 1965 American Chemical Society.

cyclic unit in the crystal structure if MOFs is common. The folded conformation of N_4 azamacrocycles is widely unobserved within reported MOF structures.

In this review, we endeavor to delineate recent advances of the fabrication of azamacrocycles into MOF structures. Furthermore, we discuss the main applications investigated using azamacrocycle-containing MOFs, which include molecular recognition and separation, template synthesis, gas adsorption, and heterogenous catalysis. The reported MOF structures have been divided by the employment of discrete transition metal–azamacrocycle complexes as organic building blocks and azamacrocyclic derivatives functionalized via N-alkylation of coordination capable pendant arms.

2. Design strategies

The prevalence of square-planar azamacrocyclic complexes have established the use of 0D complexes of popular N4-azamacrocycles, e.g. 1,4,7,10-tetrazacyclododecane (cyclen) and 1,4,8,11-tetraazacyclotetradecane (cyclam), as structure growth directors [59,62–64]. Azamacrocycles employed in this fashion are depicted in Fig. 1a. The 0D complex dictates the extension of the framework in linear fashion via coordination to the only available coordination sites at the trans-axial position, thereby simplifying the design, prediction and structure elucidation of network structures. The aforementioned describes the prevailing design methodology that governs the larger majority of reported MOF structures which combine the metal–azamacrocyclic complex with organic ligands of multidenticity to afford extended frameworks [59]. More recently, reports have arisen of structures composed using azamacrocycles functionalized via the alkylation of an appropriate pendant with a functional moiety capable of coordination at the nitrogen heteroatom of the macrocycle, which can preclude the need to employ secondary bridging ligands to form extended networks. Functionalized derivatives of azamacrocycles present two advantages to MOF synthesis; firstly, their use precludes the need of a secondary bridging ligand to produce an extended framework, and, secondly, a potential to produce MOFs with secondary porosity arising from vacant macrocycle cavities that may fully be utilized post-MOF formation [60,61].

2.1. Strategies employing discrete transition metal–azamacrocycle complexes

The earliest reported azamacrocycle-based MOF was observed by Choi et al. [65] in 1998 when employing a Ni^{II}-1,3,5,8,10,12-hexaazacyclotetradecane-3,10-diethanol macrocyclic complex with 1,3,5-benzenetricarboxylate (BTC^{3-}) in solvothermal synthetic conditions in excess pyridine (Fig. 3). The exploitation of a tricarboxylate ligand as a triangular building unit alongside a linear

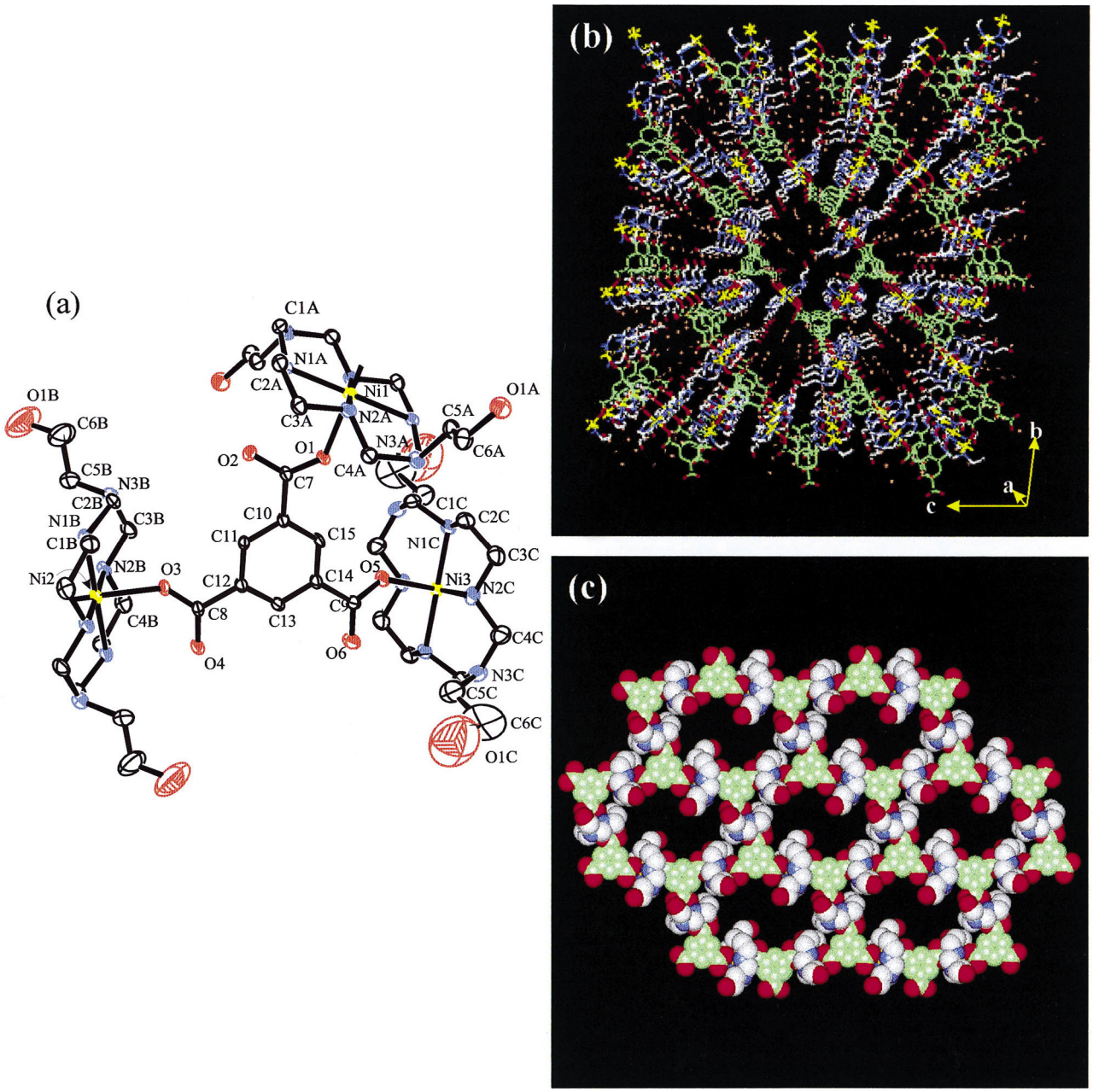

Fig. 3. Azamacrocyclic MOF formed using Ni^{II}-1,3,5,8,10,12-hexaazacyclotetradecane-3,10-diethanol macrocyclic complex with BTC^{3-} (a) ORTEP view of the trinuclear unit with atomic numbering scheme. (b) Projection along a axis, displaying honeycomb structure. (c) CPK presentation. Reprinted with permission from Ref. [65]. Copyright 1998 American Chemical Society.

linker in the form of a macrocyclic complex that exhibits a square-planar geometry will encourage the development of a 2D framework with honeycomb type cavities. Six macrocyclic complexes and six tridentate ligands constitute each cavity; wherein each Ni^{II}-azamacrocyclic complex contributes to two cavities and each BTC^{3-} contributes to three, giving a 2D network of stoichiometry M^{II}:L = 3:2. Supramolecular interlayer interactions often prompt the alignment of the pores of a 2D honeycomb framework to produce 1D channels within a pseudo-3D coordination network. Hydrogen bonding, between the macrocycle hydroxyl pendants and the amine moieties of a macrocycle in an adjacent layer, and π-π stacking interactions, between guest pyridine molecules and BTC^{3-} anions, afford 1D channels of effective cavity size of 11.4 × 11.4 $Å^2$. Like many early MOF materials, the framework undergoes structural changes upon guest removal. Self-assembly with larger tricarboxylate ligands result in framework interpenetration. In 2005, Suh et al. [66] utilized a Ni^{II}-cyclam complex in conjunction 1,3,5-tris [2-(4-carboxylphenyl)-1-ethynyl] benzene ($TCPEB^{3-}$) to produce a 2D network of threefold parallel interwoven (6,3) nets with triangular voids of effective cavity size 18.4 × 14.7 × 9.5 $Å^3$ and 35% free crystal volume.

Supramolecular interactions can also encourage 3D *pseudo*-MOF type structures from 1D coordination polymers (CPs) [59–61]. As demonstrated by Suh et al. [59], self-assembly between a Ni^{II}-cyclam complex and 2,2′-bipyridyl-5,5′-dicarboxylate ($BPyDC^{2-}$) afforded a 1D CP {Ni(cyclam)(BPyDC)]·H_2O} which forms an extended supramolecular structure in the manner of a double network of threefold braids made by CP chains extending in three different directions, aided by C–H–π interactions arising between the macrocycle and the pyridyl moieties of the ligand

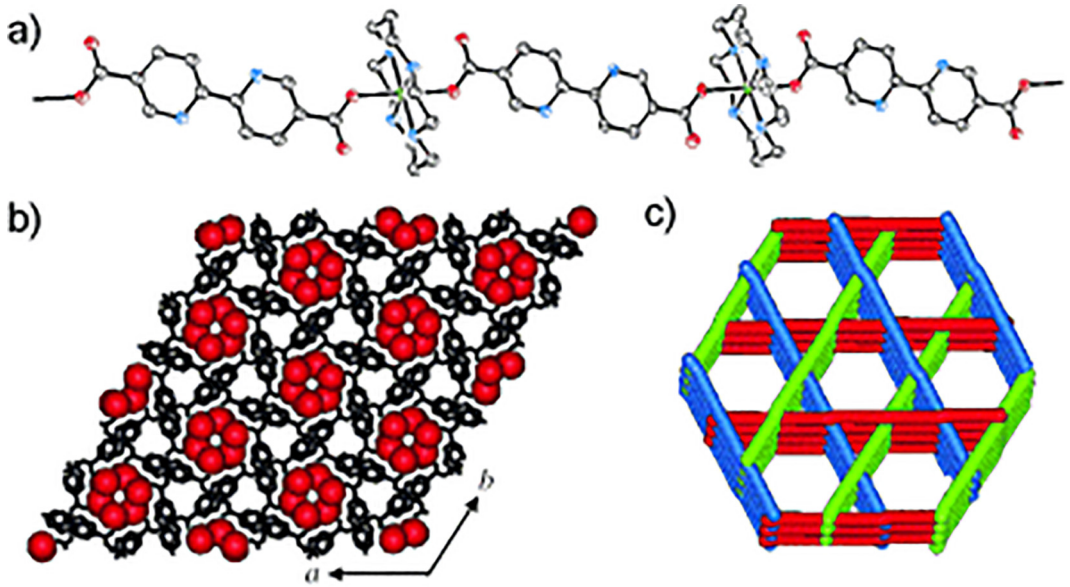

Fig. 4. X-ray structure of {Ni(cyclam)(BPyDC)]·H_2O}. (a) Structure of the linear coordination polymer. (b) View on the ab plane showing the linear coordination polymer chains extending in three directions; water guest molecules occupying the channels are depicted in CPK style (red). (c) View showing the stacking of the linear chains, which generates 1D channels. Reproduced from Ref. [59] with permission from John Wiley & Sons, Inc. (Color online.)

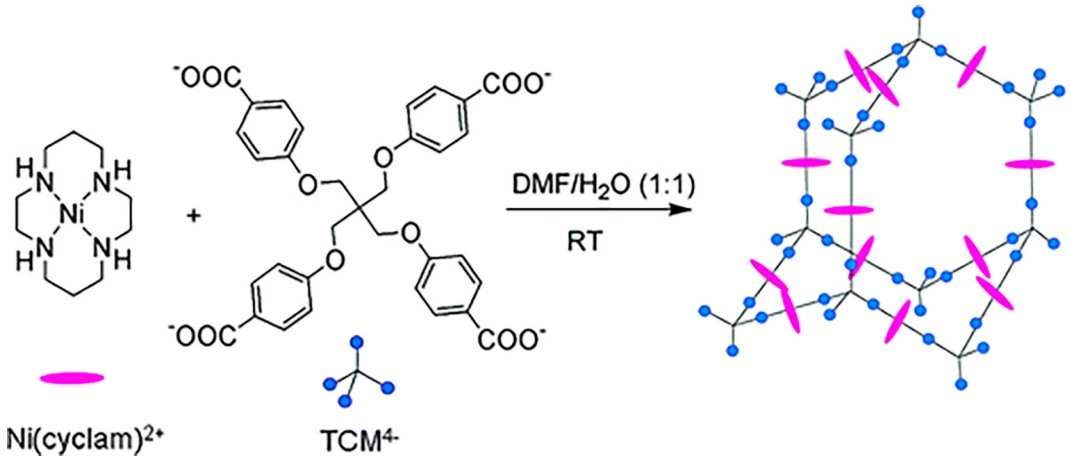

Fig. 5. Self-assembly of $[Ni(cyclam)]^{2+}$ and TCM^{4-} in DMF/water (1. 1, v/v) resulted in $[Ni(cyclam)]_2[TCM]\cdot 2DMF\cdot 10H_2O$. Reprinted with permission from Ref. [68]. Copyright 2005 American Chemical Society.

(Fig. 4). The packing results in 1D channels with honeycomb openings with an effective cavity size of 5.8 Å. Similar results were achieved with a Ni^{II}-cyclam derivative complex alongside 4,4′-biphenyldicarboxylate. The resulting framework exhibited 1D channels with honeycomb openings of an effective 7.3 Å pore size [67]. The framework displays thermal stability up to 300 °C and exhibits permanent porosity, gas storage capability, and selective guest binding properties.

Utilization of tetrahedral tetradentate bridging ligand with a metal–azamacrocycle linear linker produces a diamondoid type network with adamantoid cages. In 2005, Suh and co-workers [68] obtained a diamondoid network, $[[Ni(cyclam)](ClO_4)]_2[TCM]\cdot 2DMF\cdot 10H_2O$ from the self-assembly of tetrakis[4-(carboxyphenyl) oxamethyl] methane (TCM) with a Ni^{II}-cyclam complex (Fig. 5). The framework's large adamantanoid cages, with dimensions of 49.2 Å × 50.8 Å × 44.3 Å, prompt an 8-fold interpenetration in the [4+4] mode that generates 1D channels of a window size of 6.7 Å × 4.7 Å. The structure possesses 35% free crystal volume and thermal stability up to 300 °C; however, it displayed a lack of porosity upon guest removal yet could be restored with immersion into a H_2O:DMF solution; this flexile behavior is indicative of some MOFs employing flexible linkers.

Recently in 2016, Almáši et al. [69] were able to achieve a microporous MOF{$[Zn_2(\mu_4\text{-MTB})\ (\kappa_4\text{-cyclam})_2]\cdot 2DMF\cdot 7H_2O$} from a solvothermal reaction of methanetetrabenzoic acid (H_4MTB) and a Zn^{II}-cyclam complex, formed in-situ. The MOF displayed a fourfold interpenetrated diamondoid structure with 1D channels of sizes 14.1 × 14.1 and 2.4 × 2.4 $Å^2$. BET surface area calculations of the material gave specific surface areas 644 m^2/g (N_2) and 561 m^2/g (Ar), pore volumes 0.246 cm^3/g (N_2) and 0.239 cm^3/g (Ar), and pore size diameters of 0.65 nm (N_2) and 0.64 nm (Ar).

2.2. Strategies for functionalized derivatives of azamacrocycles

The exploitation of functionalized derivatives of azamacrocycles for MOF synthesis further increase the potential structural

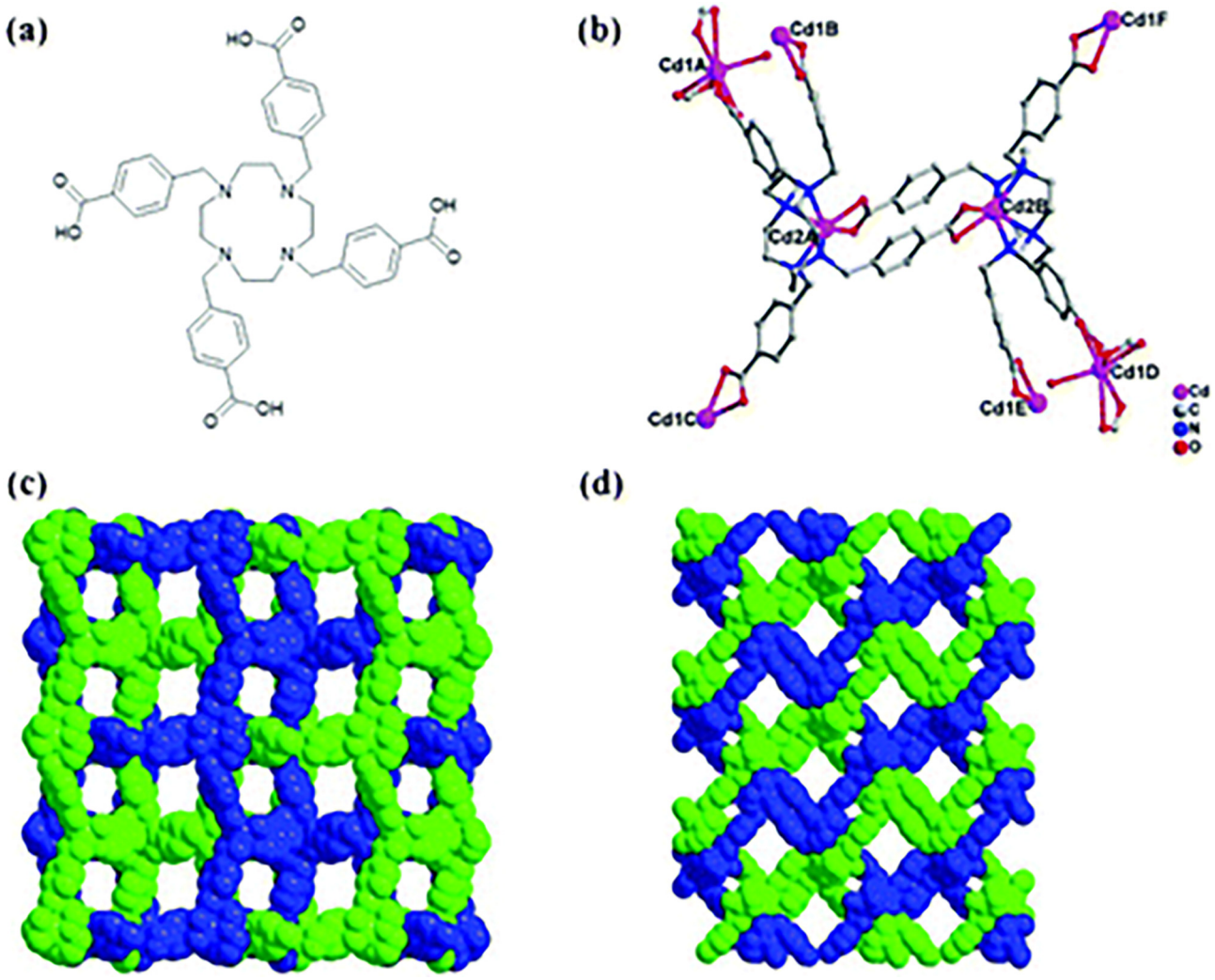

Fig. 6. (a) The tactmb ligand; (b) the coordination unit of MMCF-1; (c) the twofold interpenetrating structure viewed from the b direction; (d) the twofold interpenetrating structure viewed from the c direction. Reproduced from Ref. [72] with permission from The Royal Society of Chemistry.

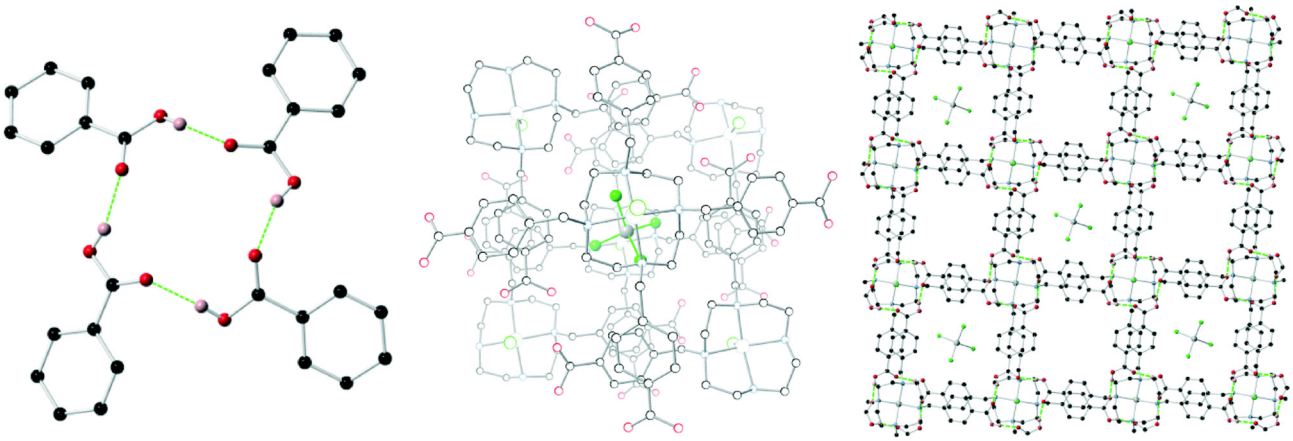

Fig. 7. Structure of $[M(H_4tactmb)Cl]_2 \cdot [MCl_4] \cdot 2EtOH$ (M = Ni, Co). Left) Diagram of the carboxylic acid tetramer hydrogen bond motif. (center) Representation of the tetrachloridonickelate anion environment within the structure, with framework atoms de-emphasized for clarity. (Right) View of two layers showing alternating incidence of tetrachloridometallate anions and cavity space containing disordered solvent. Hydrogen atoms not participating in hydrogen bonding. Reproduced from Ref. [74] with permission from The Royal Society of Chemistry.

diversity while simultaneously raising the intricacy of the design methodology describing metal–azamacrocycles as linear linkers. Synthetic modification via the direct nitrogen alkylation of the amine moiety of the macrocycle in reaction with an alkyl or benzyl halide can integrate pendant arms bearing functional moieties capable of coordination, e.g. carboxylates, phosphonate, nitriles etc

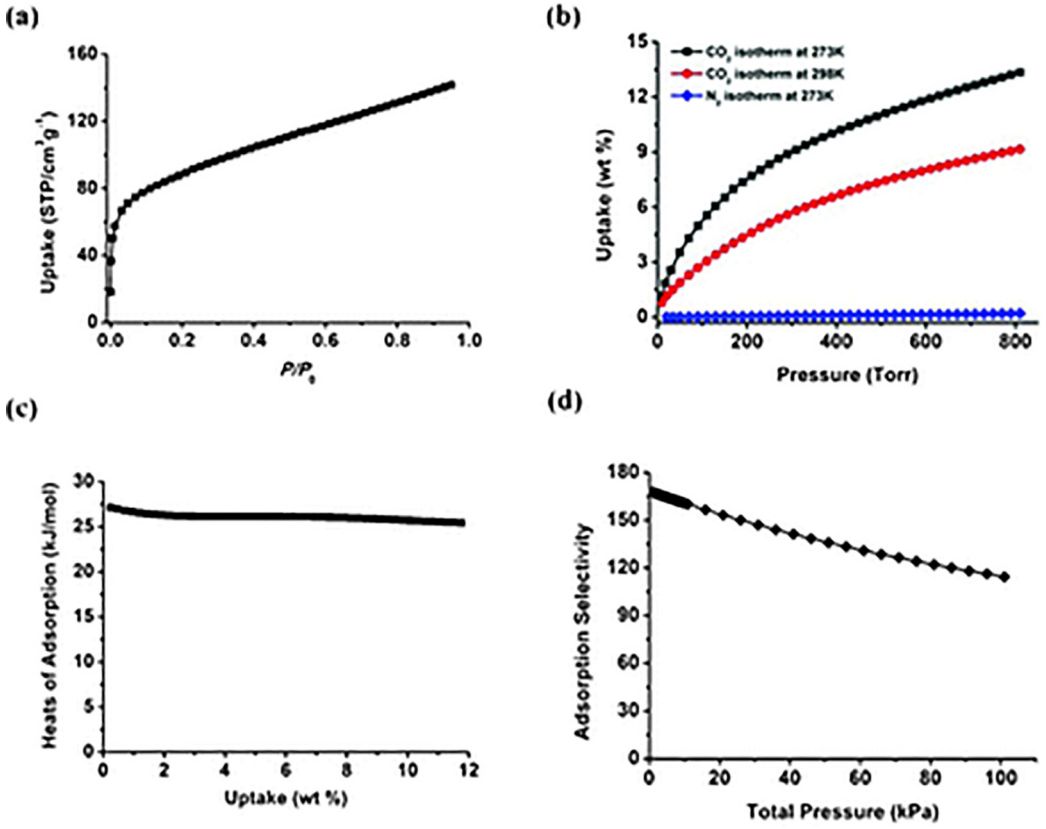

Fig. 8. (a) CO_2 adsorption isotherm of MMCF-1 at 195 K; (b) Gas a) CO_2 adsorption isotherm of MMCF-1 at 195 K; (b) Gas adsorption isotherms of MMCF-1 (black, CO_2 at 273 K; red, CO2 at 298 K; blue, N2 at 273 K); (c) heats of adsorption of CO2 for MMCF-1; (d) IAST-predicted selectivity of the mixture of CO2 and N2 for MMCF-1. Reproduced from Ref. [72] with permission from The Royal Society of Chemistry. (Color online.)

[61]. The macrocyclic ligand may now be treated as a polydentate structural building unit and often still forms a metal–azamacrocycle complex in situ or by design prior to crystallization of an extended network. The polydentate azamacrocyclic complex may then afford intriguing 3D structures through coordination of the pendant moieties to metal ions or clusters, not excluding the inter- or intramolecular interaction between the functional group and the metal–azamacrocyclic complex. Other secondary co-ligands may be introduced to further raise network complexity. Additionally, supramolecular interactions originating from hydrogen bonding between the functional moiety of the pendant arms, the amines of the macrocycle, and solvent guests, as well as, π–π interactions with aryl groups of pendant arms may also facilitate the formation of an extended 3D framework [59–61]. In comparison to the rigid type structural building unit discussed previously, these flexible type ligands offer multiple favorable conformations of similar energies to promote structural diversity yet difficult crystallization with metal ions. Thusly, there are few reported examples of MOFs employing functionalized derivatives of azamacrocycles.

In 2012, Zhu et al. [70] report using 1,4,8,11-tetraazacyclotetradecane-1,4,8,11-tetraacetic acid as a bifunctional organic linker to afford isostructural prismatic crystals of $[Eu_2Zn_3(TETA)_3(H_2O)_4]\cdot 12H_2O$ and $[Gd_2Cu_3(TETA)_3(H_2O)_2]\cdot 6H_2O$, which represent the first 3d–4f heterometallic azamacrocyclic MOFs. The frameworks feature a distorted octahedral transition metal macrocyclic complex, wherein the metal coordinates to the nitrogens of the macrocycle and two carboxylates on the pendant arms while the two other carboxylates are protonated and uninvolved in coordination. Each lanthanide ion exists in a nine-coordinate distorted tricapped triprismatic geometry; each atom coordinates to two water molecules and five $TETA^{4-}$ ligands. This gives rise to a 3D pillared-layer framework with 1D hexagonal channels with window dimensions 17.82·15.03 Å^2. In 2013, Zhu et al. [71] showed the hydrothermal reaction of Pb(II) with H_4TETA afforded a porous MOF structure $[Pb_2(TETA)]\cdot 6H_2O$. The framework exhibits a trigonal space group **R-3**. The 3D framework is formed via crosslinked 1D chains of lead atoms hexacoordinated by two carboxylate oxygens and two amine moieties from a single macrocycle ligand along with two carboxylate oxygens from two separate macrocycle moieties. Interestingly, the unoccupied macrocycle acts as a pillar linker. The framework contains 1D hexagonal channels with windows of dimensions 22.35 × 19.01 Å^2.

In 2012, our group [72] obtained a twofold interpenetrating microporous MOF (MMCF-1, Metal–Macrocyclic Framework) from the solvothermal reaction of azamacrocyclic tetracarboxylate ligand 1,4,7,10-tetraazacyclododdecane-*N*,*N*′,*N*″,*N*‴-tetra-*p*-methylbenzoic acid (tactmb) with $Cd(NO_3)_2\cdot 4H_2O$. MMCF-1 exhibits space group $P2_1/c$ with an asymmetric unit containing two unique Cd atoms; the first is seven coordinated with six oxygen atoms of three carboxylate groups from three separate ligands alongside one water molecule and the second is six-coordinated to the four nitrogens of a macrocycle and the oxygen atoms of a separate tactmb (Fig. 6). MMCF-1 possesses two types of rectangular channels of sizes 4.8 × 4.8 Å^2 and 7.5 × 8.2 Å^2, thermal stability up to 320 °C, and a BET surface area of ~500 m^2/g. The solvothermal reaction of tactmb with copper nitrate affords $[Cu_2(Cu\text{-}tactmb)(H_2O)_3(NO_3)_2]$, MMCF-2 [73], which crystallizes in the $Pm\bar{3}m$ space group. The framework exhibits an nbo topology arising from two different types of 4-connected square planar nodes, copper paddlewheels and the Cu-metallated tactmb ligand. MMCF-2 exhibits nanoscopic cuboctahedral cages with Cu^{II}-metalated azamacrocycles occupying the six square faces and paddlewheel SBUs occupying the vertices. Thermogravimetric analysis

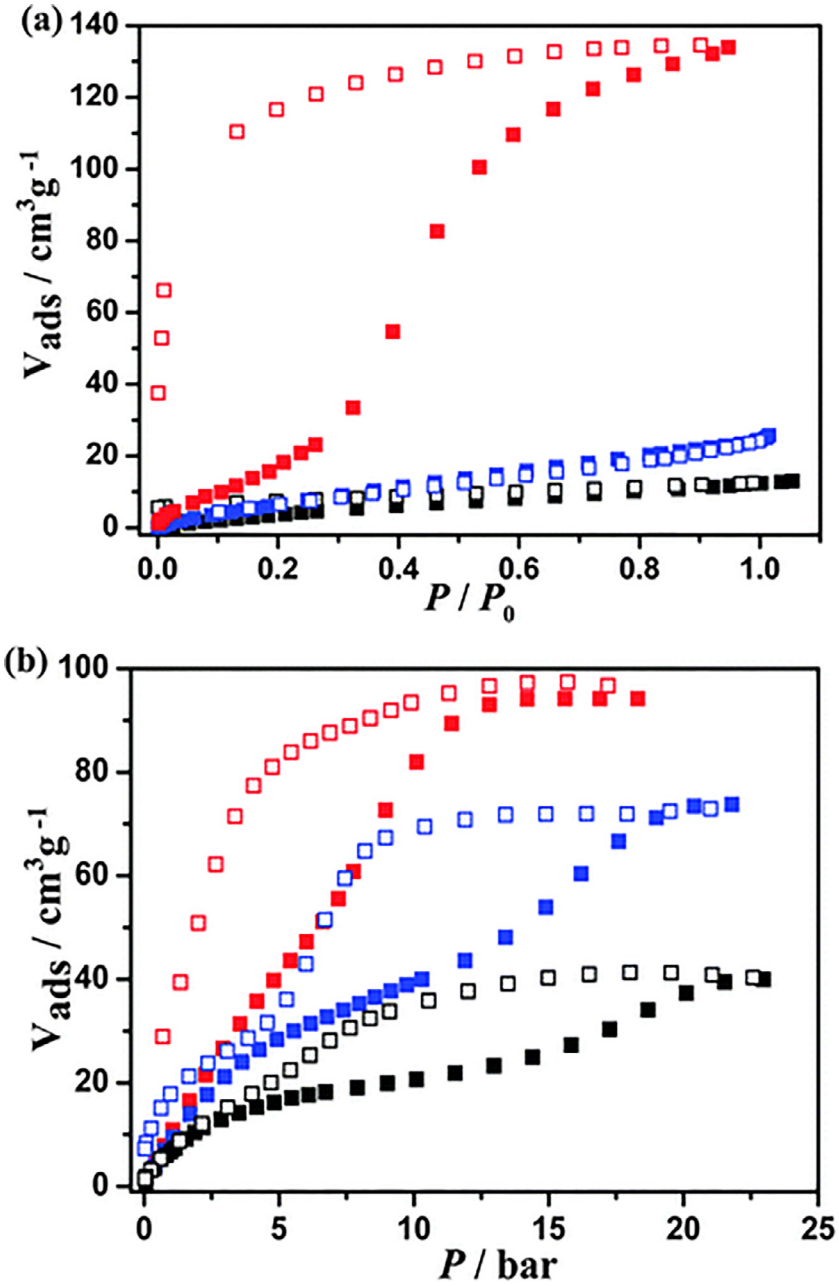

Fig. 9. (a) Gas adsorption isotherms of $[(NiL)_3(TCBA)_2]\cdot 12H_2O$ for N2 (blue) and H2 (black) at 77 K, and CO_2 (red) at 195 K. (b) CO_2 adsorption isotherms for 1d measured at 273 K (red), 298 K (blue), and 323 K (black) (the solid and hollow symbols represent adsorption and desorption. Reproduced from Ref. [88] with permission from The Royal Society of Chemistry. (Color online.)

established stability up to around 290 °C, and nitrogen adsorption studies at 77 K revealed a BET surface area of about 450 m^2/g.

In 2014, Hawes et al. [74] reacted tactmb with either nickel (II) chloride hexahydrate or cobalt (II) chloride hexahydrate to produce isostructural frameworks, $[M(H_4tactmb)Cl]_2\cdot[MCl_4]\cdot 2EtOH$ (M = Ni, Co), characterized by discrete nickel (II) and cobalt (II) macrocycle complexes that produce 2D sheets from the formation of rare hydrogen-bonded carboxylic acid tetramers with checkerboard cavities (Fig. 7). The sheets further organize into a 3D supramolecular framework due to π–π interactions between the aromatic rings of the pendant arms. The range of structural diversity and framework complexities afforded from the functionalized derivatives of azamacrocycles H_4TETA and H_4tactmb demonstrates unsuitability of design strategies applied to rigid organic struts when synthesizing MOFs.

3. Applications

3.1. Gas Adsorption and Storage

Gas adsorption and storage the hallmark high surface area and porosity of MOF materials have long been one of driving forces in the investigation of their gas sorption and storage capabilities for energy-efficient, eco-friendly adsorptive technologies [20,75–79]. Potential tunability of pore size by employing selected organic struts and catenation, as well as, modulation of framework properties through the inclusion of desired functional groups to enhance adsorption of adsorbates of interest, e.g. the greenhouse gas CO_2 whose emissions pose significant environmental and economic threats [80–82]. Incorporation of functionalities including open metal sites, such as those arising from a square planar

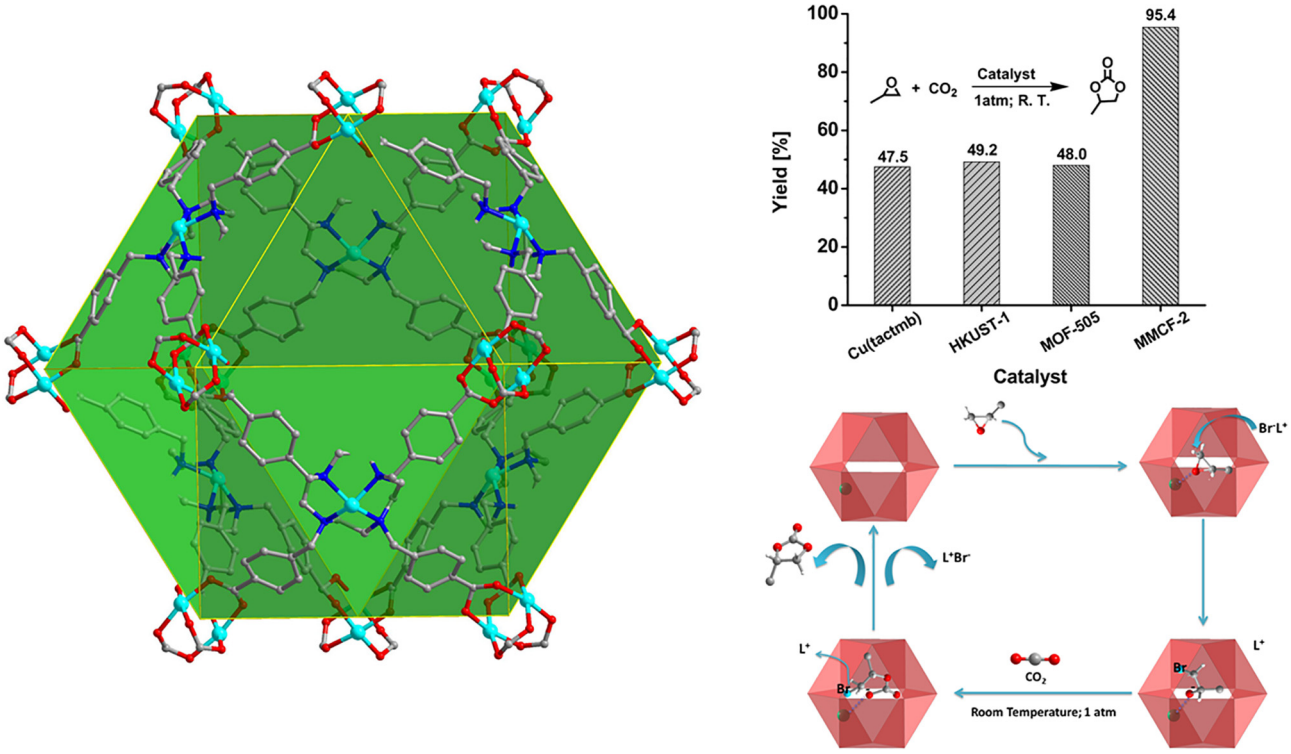

Fig. 10. (Left) The cuboctahedral cage of MMCF-2. (Top Right) A representation of the tentatively proposed catalytic mechanism for the cycloaddition of epoxide and CO_2 into cyclic carbonate catalyzed by MMCF-2 (green sphere. open metal site; L+ = tetra-*n*-tertbutylammonium). (Bottom Right) The yield of propylene carbonate from cycloaddition of propylene oxide and CO_2 catalyzed by Cu(tactmb), HKUST-1, MOF-505, and MMCF-2 after 48 h at room temperature under 1 atm CO_2 pressure. Adapted from Ref. [73] with permission from John Wiley & Sons, Inc.

metal–azamacrocycle complex, and amine groups from the macrocycle ring have been identified to increase CO_2 adsorption enthalpies [83,84]. Uptake may be further improved via in introduction of hydroxyl and alkyl halide groups [85,86].

In 2012, our group [72] demonstrated MMCF-l exhibits a CO_2 uptake capacity of 140 cm^3/g at 1 atm with type I adsorption behavior typical of microporous materials (Fig. 8). MMCF-1 evinces CO_2 uptake capacities of 13.1 wt% at 273 K and 9.0 wt% at 298 K under 1 atm of pressure, and exhibits a constant heat of adsorption (Q_{st}) of CO_2 of ~26 kJ/mol. Our group demonstrates the framework's selective capacity of 73 for CO_2/N_2 at 273 K and estimate the adsorption selectivity of CO_2 over N_2 to be 114 at 273 K, as calculated from the Ideal Adsorption Solution Theory (IAST) [87] for selectivity of CO_2/N_2 (typically 15/85%) in post-combustion flue gas streams. This selective uptake and adsorption selectivity as estimated from IAST represent the highest yet reported for azamacrocyclic-based MOFs.

MOF $[Zn_2(\mu_4\text{-MTB})(\kappa_4\text{-cyclam})_2]\cdot 2DMF\cdot 7H_2O$ [69] displayed a CO_2 uptake 54.6 cm^3/g and 10.5 wt%, as well as an Q_{st} value of 22.8 kJ/mol as calculated via the Clausius–Clapeyron equation. Hydrogen adsorption isotherms at 77 K and 87 K of $[Zn_2(\mu_4\text{-MTB})(\kappa_4\text{-cyclam})_2]\cdot 2DMF\cdot 7H_2O$ show a type I isotherm with a maximum uptake capacity 134.75 cm^3/g (1.28 wt%) and 84.17 cm^3/g (0.75 wt%), respectively. In 2013, Ju et al. [88] reported $[(NiL)_3(\text{-TCBA})_2]\cdot 12H_2O$, where L = 2-(1,3,5,8,12-pentaazacyclotetradecan-3-yl) butan-1-ol and H_3TCBA = tri(4-carboxybenzyl)amine, which assembles from fivefold interlocked nanotubes and exhibits stepwise sorption behavior for CO_2 adsorption (Fig. 9). Below 0.26 atm, the evacuated framework only captures 23 cm^3/g, and then rapidly reaches a saturation value of 134 cm^3/g (26.3 wt%) at 0.95 atm. This "gate effect" [89–91] is attributed to dynamic pores generated by the closed fivefold interlocked tubes.

The sorption characteristics of metal azamacrocyclic frameworks may be further tuned through variation in the metal identity participating in the metal–azamacrocycle complex and the placement of substituent position on aryl pendant arms. In 2013, Huang et al. [92] reported an isostructural porous MOF series$\{[M'(\text{cyclam})]_2\ [M(2,5\text{-pydc})_3]\cdot xH_2O\}_n$, where M = Co, Ni, Zn and M′ = Ni, Zn, demonstrating that complexes constructed using $[Ni(\text{cyclam})]^{2+}$ exhibit larger CO_2 sorption capacity than those using $[Zn(\text{cyclam})]^{2+}$. This may be attributed to increased interaction of coordinatively unsaturated Ni centers with CO_2 molecules.

3.2. Heterogeneous catalysis

MOF-based catalytic materials show several advantages over other porous material based catalysts: firstly, high surface area to facilitate the contact between substrates and the catalytic active site, resulting in improved catalytic reactivity; secondly, relative uniformity and tunability of framework pores assist the catalytic selectivity of substrate; and finally, facile functionalization and incorporation of catalytic active sites into MOFs permit the manipulation of the nano-environment to further enhance catalytic activity [93]. MMCF-2 [73] demonstrated highly efficient catalytic activity for the cycloaddition reaction of propylene oxide with carbon dioxide into propylene carbonate at room temperature under 1 atm CO_2 pressure obtaining a yield of 95.4% over 48 h (Fig. 10). The catalytic activity is nearly twice that of homogeneous Cu(tactmb) (47.5%), cubeoctahedral MOF-505 [94] (48.0%) and the benchmark polyhedral cage-containing copper MOF, HKUST-1 (49.2%). The high activity for the fixation of CO_2 under ambient conditions may be attributed to the high density of active sites, many of which are favorably oriented in the octahedral cage.

In 2016, Martín-Caballero et al. [95] reported the decavanadate-based microporous MOF $[Cu(\text{cyclam})]$ $[\{Cu(\text{cyclam})\}_2(V_{10}O_{28})]\cdot 10H_2O$ exhibited significant activity as an heterogenous catalyst intended for the peroxide-based oxidation of adamantane. The catalyst remarkably achieved 99% conversion after only 6 h with low

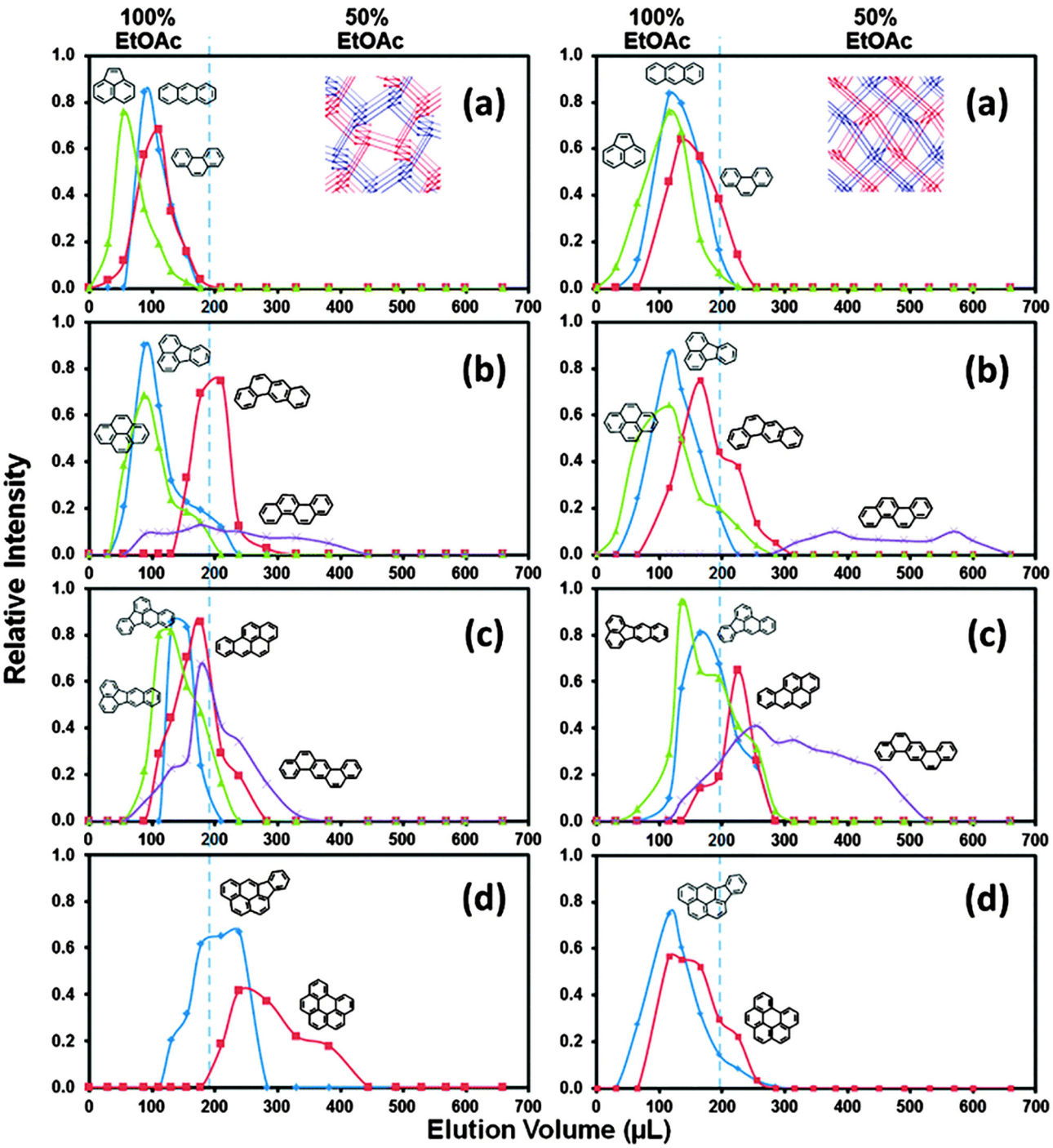

Fig. 11. Elution profiles of PAHs with 3–6 aromatic rings using stationary phases 1A (left) and 1B (right). Inset. topological representations of MOFs 1A and 1B. Listed compounds are in the order of elution for each set. From left to right. (a) Acenaphthylene, anthracene, phenanthrene; (b) pyrene, fluoranthene, benz[a]anthracene, chrysene; (c) benzo[k]fluoranthene, benzo[b]fluoranthene, benzo[a]pyrene, dibenz[a,h]anthracene; (d) indeno[1,2,3-cd]-pyrene, benzo[ghi]-perylene. Reproduced from Ref. [96] with permission from The Royal Society of Chemistry.

to moderate product selectivity toward 1-adamantanol over other products.

3.3. Molecular recognition and separations

Similarly, to other macrocyclic-based MOF, azamacrocyclic frameworks potentially possess two levels of porosity arising from the porous MOF structure and rarely observed cavities of the macrocycle. This hierarchical porosity lends a capacity to recognize small molecules suggesting potential applications in chromatographic separation and sensing [61]. In 2014, Hawes et al. [96] reported the capabilities of two phases of MMCF-1 for the separation of complex mixtures of polycyclic aromatic hydrocarbons (PAHs) and polar compounds. Both phases are porous, interpenetrated 3D frameworks that only differ in topology due to positioning of the benzoate pendant arms, resulting in ins- and kdd-related nets. The phases offered an opportunity to showcase size-selective separation capability; both had very similar surface polarities but

differed by void volumes and channel diameters, 14 Å (ins) and 11 Å (kdd). Small-scale separation experiments utilizing a mixture of 16 PAH compounds selected as size selectivity analyte probes and another mixture of 9 compounds of disparate polarity to examine polar and coordination interactions. The ins phase displayed the highest retention values for larger analytes. In contrast, the kdd phase had enhanced separation of 4 and 5 aromatic ring analytes. The phases share enhanced retention with increasing analyte dipole moment. Hydrogen-bonding interactions further increase further improve retention (Fig. 11).

In 2016, Gurtovyi et al. demonstrated the use of the bimodal luminescence arising from loading the Zn-MOF {[Zn(cyclen)(4,4′-diphenyldicarboxylate)]·0.4DMF·1.7H_2O}$_n$ with a dopant organic dye acridine orange, which featured overlap between the dye's absorption band (λ_{max} = 500 nm) and the MOF emission band [97]. Immersion in nitrobenzene dissolved in hexane selectively quenched emission arising from the MOF; however, nitrobenzene and 2-nitrotoluene vapor quenched the luminescence of the organic dye [98]. The attainment of azamacrocyclic MOF materials which retain hierarchical porosity, i.e. porosity arising from the pore and channels of the framework alongside vacant macrocycle site, further increase the utility of these materials in recognition applications. Yet, only a very few instances hierarchical porosity in azamacrocyclic based MOFs have been reported [71,99]. Investigations of the properties of these frameworks are still needed.

3.4. Other applications

The strong metal complexation and ability to form thermodynamically stable complexes of azamacrocycle ligands has promoted their usage as MRI contrast agents [100–102]. In 2013, Maspoch et al. [102] utilized the azamacrocyclic ligand 1,4,7,10-tetraaza-cyclododecane-1,4,7,10-tetramethylene-phosphonic acid to produce the bimetallic MOF [GdCu(DOTP)Cl]·4.5H_2O. Relaxometry studies show a non-pH dependent maximum in r_1 relaxivity of 15 mM^{-1} s^{-1} at 40 MHz and at high field (500 MHz) r_1 = 5 mM^{-1} s^{-1}. The potential contrast agent was reportedly stable in both physiological saline solution and cell culture media, not cytotoxic, and miniaturizable to the nanoscale as stable colloids.

4. Conclusion

The presented data demonstrates breadth of diversity of azamacrocyclic-based MOFS. Specifically, we detail strategies and techniques developed thus far to incorporate azamacrocycles within a single framework with the hopes these strategies are enhanced and applied to develop novel systems, including functionalized derivatives of these macrocycles. The data may be fragmented due to the scarcity of this class of porous materials but shows the promise of these materials in numerous applications; such as molecular recognition, separation, sensing, gas storage and adsorption.

The inclusion of azamacrocycles into MOF materials combine the characteristic high thermodynamic stability, basicity, and strong metal complexation of the macrocycles with the high porosity, surface area, and tunability of the frameworks. Full realization of the potential of Azamacrocyclic-based MOFs requires the preparation of new entrants to this class of materials that espouse various topological structures while incorporating diverse azamacrocycles. It has been shown that the hierarchical porosity associated with macrocyclic based frameworks can be obtained using this class of ligands [71,99]. The development of more frameworks exhibiting this characteristic is needed to fully investigate the potential applications of MOFs retaining the vacant cavities of the azamacrocycles. Effectuation of hierarchical porosity of azamacrocyclic frameworks will broaden sensing applications, e.g. azamacrocycles have performed as receptors of anions, cations, amino acids and other analyte molecules, and provide an ideal slot to integrate open metal site into MOFs.

Acknowledgments

This work was supported by the National Science Foundation under Grant DMR-1352065.

References

[1] H.-C. Zhou, J.R. Long, O.M. Yaghi, Chem. Rev. 112 (2012) 673.
[2] H. Furukawa, K.E. Cordova, M. O'Keeffe, O.M. Yaghi, Science 341 (2013) 1230444.
[3] G. Férey, Chem. Soc. Rev. 37 (2008) 191.
[4] S. Kitagawa, R. Kitaura, S.-I. Noro, Angew. Chem., Int. Ed. 43 (2004) 2334.
[5] L.J. Murray, M. Dinca, J.R. Long, Chem. Soc. Rev. 38 (2009) 1294.
[6] J.-R. Li, J. Sculley, H.-C. Zhou, Chem. Rev. 112 (2012) 869.
[7] H. Wu, Q. Gong, D. Olson, H. Li, J. Chem. Rev. 112 (2012) 836.
[8] Q.-L. Zhu, Q. Xu, Chem. Soc. Rev. 43 (2014) 5468.
[9] J.-P. Zhang, X.-C. Huang, X.-M. Chen, Chem. Soc. Rev. 38 (2009) 2385.
[10] W.-Y. Gao, M. Chrzanowski, S. Ma, Chem. Soc. Rev. 43 (2014) 5841.
[11] S. Ma, H.-C. Zhou, Chem. Commun. 46 (2010) 44.
[12] K. Sumida, D.L. Rogow, J.A. Mason, T.M. McDonald, E.D. Bloch, Z.R. Herm, T.-H. Bae, J.R. Long, Chem. Rev. 112 (2012) 724.
[13] M.P. Suh, H.J. Park, T.K. Prasad, D.-W. Lim, Chem. Rev. 112 (2012) 782.
[14] Y. He, W. Zhou, G. Qian, B. Chen, Chem. Soc. Rev. 43 (2014) 5657.
[15] S. Qiu, M. Xue, G. Zhu, Chem. Soc. Rev. 43 (2014) 6116.
[16] J.Y. Lee, O.K. Farha, J. Roberts, K.A. Scheidt, S.T. Nguyen, J.T. Hupp, Chem. Soc. Rev. 38 (2009) 1450.
[17] M. Yoon, R. Srirambalaji, K. Kim, Chem. Rev. 112 (2012) 1196.
[18] J. Liu, L. Chen, H. Cui, J. Zhang, L. Zhang, C.-Y. Su, Chem. Soc. Rev. 43 (2014) 6011.
[19] L. Ma, C. Abney, W. Lin, Chem. Soc. Rev. 38 (2009) 1248.
[20] M.D. Allendorf, C.A. Bauer, R.K. Bhakta, R.J.T. Houk, Chem. Soc. Rev. 38 (2009) 1330.
[21] Z. Hu, B.J. Deibert, J. Li, Chem. Soc. Rev. 43 (2014) 5815.
[22] L.E. Kreno, K. Leong, O.K. Farha, M. Allendorf, R.P. Van Duyne, J.T. Hupp, Chem. Rev. 112 (2012) 1105.
[23] P. Ramaswamy, N.E. Wong, G.K.H. Shimizu, Chem. Soc. Rev. 43 (2014) 5913.
[24] J.M. Taylor, R.K. Mah, I.L. Moudrakovski, C.I. Ratcliffe, R. Vaidhyanathan, G.K. Shimizu, J. Am. Chem. Soc. 132 (2010) 14055.
[25] J.A. Hurd, R. Vaidhyanathan, V. Thangadurai, C.I. Ratcliffe, I.L. Moudrakovski, G.K.H. Shimizu, Nat. Chem. 1 (2009) 705.
[26] T. Yamada, K. Otsubo, R. Makiura, H. Kitagawa, Chem. Soc. Rev. 42 (2013) 6655.
[27] P. Horcajada, R. Gref, T. Baati, P.K. Allan, G. Maurin, P. Couvreur, G. Férey, R.E. Morris, C. Serre, Chem. Rev. 112 (2012) 1232.
[28] P. Horcajada, T. Chalati, C. Serre, B. Gillet, C. Sebrie, T. Baati, J.F. Eubank, D. Heurtaux, P. Clayette, C. Kreuz, J.-S. Chang, Y.K. Hwang, V. Marsaud, P.-N. Bories, L. Cynober, S. Gil, G. Féirey, P. Couvreur, R. Gref, Nat. Mater. 9 (2010) 172.
[29] J.D. Rocca, D. Liu, W. Lin, Acc. Chem. Res. 44 (2011) 957.
[30] M. Yoon, K. Suh, S. Natarajan, K. Kim, Angew. Chem., Int. Ed. 52 (2013) 2688.
[31] T.R. Cook, Y.R. Zheng, P.J. Stang, Chem. Rev. 113 (2013) 734.
[32] I.V. Perry, J.J.T. Perman, M.J. Zaworotko, Chem. Soc. Rev. 38 (2009) 1400.
[33] S.M. Cohen, Chem. Rev. 112 (2012) 970.
[34] P. Deria, J.E. Mondloch, O. Karagiaridi, W. Bury, J.T. Hupp, O.K. Farha, Chem. Soc. Rev. 43 (2014) 5896.
[35] J.D. Evans, C.J. Sumby, C.J. Doonan, Chem. Soc. Rev. 43 (2014) 5933.
[36] Z. Wang, S.M. Cohen, Chem. Soc. Rev. 38 (2009) 1315.
[37] K.K. Tanabe, S.M. Cohen, Chem. Soc. Rev. 40 (2011) 498.
[38] B. Li, Y. Zhang, D. Ma, T. Ma, Z. Shi, S. Ma, J. Am. Chem. Soc. 136 (2014) 1202.
[39] Z. Zhang, L. Wojtas, M. Eddaoudi, M.J. Zaworotko, J. Am. Chem. Soc. 135 (2013) 5982.
[40] Z. Zhang, W.-Y. Gao, L. Wojtas, S. Ma, M. Eddaoudi, M.J. Zaworotko, Angew. Chem., Int. Ed. 51 (2012) 9330.
[41] M.H. Alkordi, Y. Liu, R.W. Larsen, J.F. Eubank, M. Eddaoudi, J. Am. Chem. Soc. 130 (2008) 12639.
[42] V. Lykourinou, Y. Chen, X.-S. Wang, L. Meng, T. Hoang, L.-J. Ming, R.L. Musselman, S. Ma, J. Am. Chem. Soc. 133 (2011) 10382.
[43] Y. Chen, V. Lykourinou, C. Vetromile, T. Hoang, L.-J. Ming, R.W. Larsen, S. Ma, J. Am. Chem. Soc. 134 (2012) 13188.
[44] Y. Chen, V. Lykourinou, T. Hoang, L.-J. Ming, S. Ma, Inorg. Chem. 51 (2012) 9156.
[45] H. Deng, S. Grunder, K.E. Cordova, C. Valente, H. Furukawa, M. Hmadeh, F. Gándara, A.C. Whalley, Z. Liu, S. Asahina, H. Kazumori, M. O'Keeffe, O. Terasaki, J. Fraser Stoddart, O.M. Yaghi, Science 336 (2012) 1018.
[46] A. Dhakshinamoorthy, H. Garcia, Chem. Soc. Rev. 41 (2012) 5262.
[47] M. Meilikhov, K. Yusenko, D. Esken, S. Turner, G.V. Tendeloo, R.A. Fischer, J. Eur, Inorg. Chem. (2010) 3701.

[48] H.R. Moon, D.-W. Lim, M.P. Suh, Chem. Soc. Rev. 42 (2013) 1807.
[49] G. Férey, C. Mellot-Draznieks, C. Serre, F. Millange, J. Dutour, S. Surblé, I. Margiolaki, Science 309 (2005) 2040.
[50] J. Song, Z. Luo, D.K. Britt, H. Furukawa, O.M. Yaghi, K.I. Hardcastle, C.L. Hill, J. Am. Chem. Soc. 133 (2011) 16839.
[51] C.-Y. Sun, S.-X. Liu, D.-D. Liang, K.-Z. Shao, Y.-H. Ren, Z.-M. Su, J. Am. Chem. Soc. 131 (2009) 1883.
[52] M. O'Keeffe, O.M. Yaghi, Chem. Rev. 112 (2012) 675.
[53] W. Lu, Z. Wei, Z.-Y. Gu, T.-F. Liu, J. Park, J. Park, J. Tian, M. Zhang, Q. Zhang, T. Gentle III, M. Bosch, H.-C. Zhou, Chem. Soc. Rev. 43 (2014) 5561.
[54] H.-L. Jiang, T.A. Makal, H.-C. Zhou, Coord. Chem. Rev. 257 (2013) 2232.
[55] V. Guillerm, D. Kim, J.F. Eubank, R. Luebke, X. Liu, K. Adil, M.S. Lah, M. Eddaoudi, Chem. Soc. Rev. 43 (2014) 6141.
[56] M. Eddaoudi, D.F. Sava, J.F. Eubank, K. Adil, V. Guillerm, Chem. Soc. Rev. 44 (2015) 228.
[57] M.P. Suh, W. Shin, H. Kim, C.H. Koo, Inorg. Chem. 26 (1987) 1846.
[58] M.P. Suh, Adv. Inorg. Chem. 44 (1996) 93.
[59] E.Y. Lee, M.P. Suh, Angew. Chem., Int. Ed. 43 (2004) 2798.
[60] M.P. Suh, H.R. Moon, Adv. Inorg. Chem. 59 (2006) 39.
[61] H. Zhang, R. Zou, Y. Zhao, Coord. Chem. Rev. 292 (2015) 74.
[62] M. Bakaj, M.J. Zimmer, Mol. Struct. (1999) 59.
[63] B. Bosnich, C.K. Poon, M.L. Tobe, Inorg. Chem. 4 (8) (1965) 1102.
[64] Y.D. Lampeka, L.V. Tsymbal, Theor. Exp. Chem. 40 (2004) 345.
[65] H.J. Choi, M.P. Suh, J. Am. Chem. Soc. 120 (1998) 10622.
[66] M.P. Suh, H.J. Choi, S.M. So, B.M. Kim, Inorg. Chem. 42 (2003) 676.
[67] H.R. Moon, J.H. Kim, M.P. Suh, Angew. Chem., Int. Ed. 44 (2005) 1261.
[68] H. Kim, M.P. Suh, Inorg. Chem. 44 (2005) 810.
[69] M. Almáši, V. Zeleňák, A. Zukal, J. Kuchára, J. Čejkab, Dalton Trans. 45 (2016) 1233.
[70] X.-D. Zhu, Z.-J. Lin, T.-F. Liu, B. Xu, R. Cao, Cryst. Growth Des. 12 (2012) 4708.
[71] X. Zhu, T.-X. Tao, W.-X. Zhou, F.-H. Wang, R.-Mei Liu, L. Liu, Yi-Q. Fu, Inorg. Chem. Comm. 40 (2014) 116–119.
[72] W.-Y. Gao, Y. Niu, Y. Chen, L. Wojtas, J. Cai, Y.-S. Chen, S. Ma, CrystEngComm 14 (2012) 6115.
[73] W.-Y. Gao, Y. Chen, Y. Niu, K. Williams, L. Cash, P.J. Perez, L. Wojtas, J. Cai, Y.-S. Chen, S. Ma, Angew. Chem., Int. Ed. 53 (2014) 2615–2619.
[74] C.S. Hawes, S.R. Batten, D.R. Turner, CrystEngComm 16 (2014) 3737.
[75] B.A. Al-Maythalony, O. Shekhah, R. Swaidan, Y. Belmabkhout, I. Pinnau, M. Eddaoudi, J. Am. Chem. Soc. 137 (2015) 1754.
[76] W.M. Bloch, R. Babarao, M.R. Hill, C.J. Doonan, C.J. Sumby, J. Am. Chem. Soc. 135 (2013) 10441.
[77] J.J. Gassensmith, H. Furukawa, R.A. Smaldone, R.S. Forgan, Y.Y. Botros, O.M. Yaghi, J. Fraser Stoddart, J. Am. Chem. Soc. 133 (2011) 15312.
[78] Z.R. Herm, J.A. Swisher, B. Smit, R. Krishna, J.R. Long, J. Am. Chem. Soc. 133 (2011) 5664.
[79] J. An, N.L. Rosi, J. Am. Chem. Soc. 132 (2010) 5578.
[80] Y. Zhang, B. Li, K. Williams, W.-Y. Gao, S. Ma, Chem. Commun. 49 (2013) 10269.
[81] W. Lu, J.P. Sculley, D. Yuan, R. Krishna, Z. Wei, H.-C. Zhou, Angew. Chem., Int. Ed. 51 (2012) 7480.
[82] W. Lu, D. Yuan, J. Sculley, D. Zhao, R. Krishna, H.-C. Zhou, J. Am. Chem. Soc. 133 (2011) 18126.
[83] L.-C. Lin, J. Kim, X. Kong, E. Scott, T.M. McDonald, J.R. Long, J.A. Reimer, B. Smit, Angew. Chem., Int. Ed. 52 (2013) 4410.
[84] X. Kong, E. Scott, W. Ding, J.A. Mason, J.R. Long, J.A. Reimer, J. Am. Chem. Soc. 134 (2012) 14341.
[85] F. Debatin, A. Thomas, A. Kelling, N. Hedin, Z. Bacsik, I. Senkovska, S. Kaskel, M. Junginger, H. Müller, U. Schilde, C. Jäger, A. Friedrich, H.-J. Holdt, Angew. Chem., Int. Ed. 49 (2010) 1258.
[86] J.-B. Lin, J.-P. Zhang, X.-M. Chen, J. Am. Chem. Soc. 132 (2010) 6654.
[87] A.L. Myers, J.M. Prausnitz, AIChE J. 11 (1965) 121.
[88] P. Ju, L. Jiang, T.-B. Lu, Chem. Commun. 49 (2013) 1820.
[89] J. Seo, R. Matsuda, H. Sakamoto, C. Bonneau, S. Kitagawa, J. Am. Chem. Soc. 131 (2009) 12792.
[90] D. Tanaka, K. Nakagawa, M. Higuchi, S. Horike, Y. Kubota, T.C. Kobayashi, M. Takata, S. Kitagawa, Angew. Chem. 120 (2008) 3978.
[91] S. Henke, R. Schmid, J.D. Grunwaldt, R.A. Fischer, Chem. Eur. J. 16 (2010) 14296.
[92] S.-L. Huang, L. Zhang, Y.-J. Lin, G.-X. Jin, CrystEngComm 15 (2013) 78.
[93] B. Li, M. Chrzanowksi, Y. Zhang, S. Ma, Coord. Chem. Rev. 307 (2016) 106.
[94] B. Chen, N.W. Ockwig, A.R. Millward, D.S. Conteras, O.M. Yaghi, Angew. Chem. 117 (2005) 4823.
[95] J. Martin-Caballero, A. San Jose Wery, S. Reinoso, B. Artetxe, L. San Felices, B. El Bakkali, G. Trautwein, J. Alcaniz-Monge, J.L. Vilas, J.M. Gutierrez-Zorrilla, Inorg. Chem. 55 (2016) 4970–4979.
[96] C.S. Hawes, Y. Nolvachai, C. Kulsing, G.P. Knowles, A.L. Chaffee, P.J. Marriott, S. R. Batten, D.R. Turner, Chem. Commun. 50 (2014) 3735.
[97] R.I. Gurtovyi, L.V. Tsymbal, S. Shova, Y.D. Lampeka, Theor. Exp. Chem. 52 (2016) 44.
[98] R.I. Gurtovyi, Y.D. Lampeka, Theor. Exp. Chem. 52 (2016) 240.
[99] C. Stackhouse, W.-Y. Gao, L. Wojitas, W. Zhang, S. Ma, J. Coord. Chem. 69 (2016) 1844.
[100] S.J. Dorazio, A.O. Olatunde, P.B. Tsitovich, J.R. Morrow, J. Biol. Inorg. Chem. 19 (2014) 191.
[101] T.A. Kaden, Pure Appl. Chem. 65 (1999) 1477.
[102] A. Carné-Sánchez, C.S. Bonnet, I. Imaz, J. Lorenzo, É. Tóth, D. Maspoch, J. Am. Chem. Soc. 135 (2013) 17711.